

Study of $B \rightarrow \chi_{cJ} X$ at BelleV. BHARDWAJ¹

*Department of Physics and Astronomy
University of South Carolina, Columbia, SC 29208, USA*

In spite of the fact that the two-body B decays into χ_{c2} such as $B \rightarrow \chi_{c2} K^{(*)}$ are suppressed by the QCD factorization effect, the inclusive $B \rightarrow \chi_{c2} X$ branching fraction amounts to one third of the non-suppressed $B \rightarrow \chi_{c1} X$ decays because of the decay modes to the multi-body final states. Using a large statistics $\Upsilon(4S)$ data sample corresponding to 772 million B meson pairs accumulated by the Belle detector at the KEKB e^+e^- collider, precise measurements of inclusive $B \rightarrow \chi_{c1}$ and χ_{c2} branching fractions are carried out. The multi-body final states such as $\chi_{cJ} K \pi$, $\chi_{cJ} K \pi \pi$ and so on are also investigated to look for new charmonium-like resonance.

PRESENTED AT

The 7th International Workshop on Charm Physics
(CHARM 2015)
Detroit, MI, 18-22 May, 2015

¹Speaker on behalf of Belle Collaboration, supported by U.S. Department of Energy.

1 Introduction

Inclusive production of χ_{c2} mesons in B decays is relatively large [1, 2] in spite of the fact that two-body B decays into χ_{c2} are highly suppressed [3, 4, 5] (due to the angular momentum conservation). Differential branching fraction ($D\mathcal{B}$) in bins of χ_{cJ} ($J = 1, 2$) [6] suggests that χ_{c2} is found to be coming from three-body or higher multiplicity decays [1, 2], which have not been studied in detailed yet. More experimental input is needed to study these multi-body decay modes.

Study of more than three-body B decay modes with χ_{c1} and χ_{c2} in final state not only help in understanding B meson decays but also provide portal to search for charmonium/charmonium-like exotic states in one of the intermediate final states. For example, looking at the $\chi_{c1}\pi^+\pi^-$ invariant mass spectrum in $B \rightarrow \chi_{c1}\pi^+\pi^-K$ decays, one can search for $\chi_{c1}(2P)$ and/or $X(3872)$.

Using the $\chi_{cJ} \rightarrow J/\psi\gamma$ modes, we report on the inclusive branching fraction (\mathcal{B}) of $B \rightarrow \chi_{cJ}X$ decays. To further understand χ_{c1} and χ_{c2} production in B decays, we reconstruct the following exclusive B decays: $B^0 \rightarrow \chi_{cJ}\pi^-K^+$, $B^+ \rightarrow \chi_{cJ}\pi^+K_S^0$, $B^+ \rightarrow \chi_{cJ}\pi^0K^+$, $B^+ \rightarrow \chi_{cJ}\pi^+\pi^-K^+$ and $B^0 \rightarrow \chi_{cJ}\pi^+\pi^-K_S^0$ [7].

2 Data sample and event selection

We use a data sample of 772×10^6 $B\bar{B}$ events collected with the Belle detector [8] at the KEKB asymmetric-energy e^+e^- collider [9] operating at the $\Upsilon(4S)$ resonance. All results presented here are preliminary.

The J/ψ meson is reconstructed via its decays to $\ell^+\ell^-$ ($\ell = e$ or μ). To reduce the radiative tail in the e^+e^- mode, the four-momenta of all photons within 50 mrad with respect to the original direction of the e^+ or e^- tracks are included in the invariant mass calculation, hereinafter denoted as $M_{e^+e^-(\gamma)}$. The reconstructed invariant mass of the J/ψ candidates is required to satisfy $2.95 \text{ GeV}/c^2 < M_{e^+e^-(\gamma)} < 3.13 \text{ GeV}/c^2$ or $3.03 \text{ GeV}/c^2 < M_{\mu^+\mu^-} < 3.13 \text{ GeV}/c^2$. For the selected J/ψ candidates, a vertex-constrained fit is applied and then a mass-constrained fit is performed in order to improve the momentum resolution.

The χ_{c1} and χ_{c2} candidates are reconstructed by combining J/ψ candidates with a photon having energy (E_γ) larger than 100 MeV in the laboratory frame. To reduce the combinatorial background coming from $\pi^0 \rightarrow \gamma\gamma$, we use a likelihood function that distinguishes an isolated photon from π^0 decays using the photon pair invariant mass, photon laboratory energy and polar angle [10]. We reject both γ 's in the pair if the π^0 likelihood probability is larger than 0.3 (0.8) for an inclusive study ($B \rightarrow \chi_{cJ}K\pi$, $B \rightarrow \chi_{cJ}K\pi\pi$ decay modes).

3 Inclusive B decays to χ_{cJ}

To identify the signal, we use the $J/\psi\gamma$ invariant mass $M_{J/\psi\gamma}$ distribution and extract the signal yield from a binned maximum likelihood fit. A double-sided Crystal Ball function is used to model the signal shapes of $B \rightarrow \chi_{c1}X$ and $B \rightarrow \chi_{c2}X$. Figure 1 (a) shows the fit to the $M_{J/\psi\gamma}$ distribution for $B \rightarrow \chi_{c1}X$ and $B \rightarrow \chi_{c2}X$ decays.

The reconstruction efficiencies for the inclusive $B \rightarrow \chi_{c1}X$ and $B \rightarrow \chi_{c2}X$ decays are estimated to be 24.2% and 25.9%, respectively. Uncertainty on the efficiency is estimated to be 4.0%.

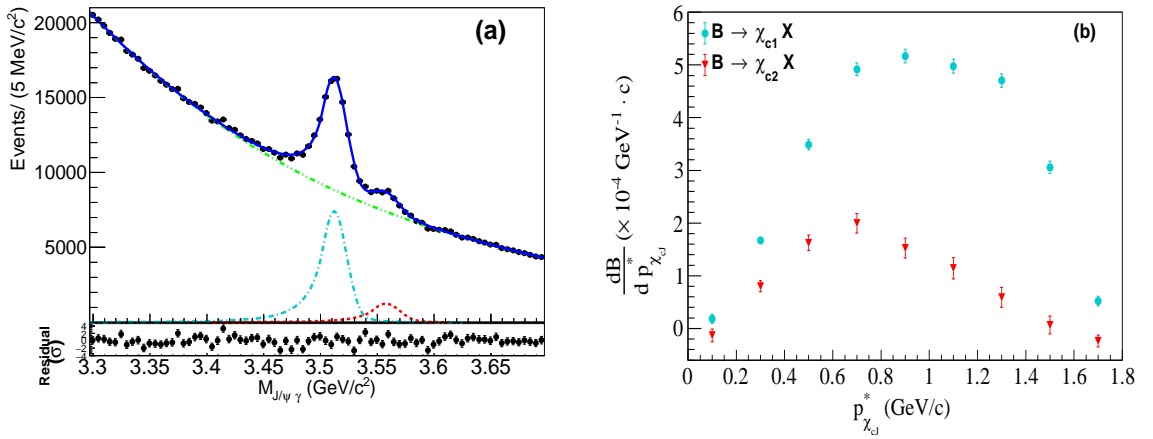


Figure 1: (a) $M_{J/\psi\gamma}$ distribution of the $B \rightarrow \chi_{cJ}(\rightarrow J/\psi(\rightarrow \ell^+\ell^-)\gamma)X$ decays in data. The curves show the signal (cyan dash-dotted for χ_{c1} and red dashed for χ_{c2}) and the background component (green dash-double-dotted for combinatorial) as well as the overall fit (blue solid). The lower plot shows the pull of the residuals with respect to the fit. (b) Plots showing $D\mathcal{B}(B \rightarrow \chi_{c1}X)$ and $D\mathcal{B}(B \rightarrow \chi_{c2}X)$ in each bin of $p_{\chi_{cJ}}^*$ for $B \rightarrow \chi_{cJ}(\rightarrow J/\psi\gamma)X$. These plots are without feed-down subtraction. The uncertainty shown in these plots are statistical only.

After subtracting the ψ' feed-down contribution, we get the direct branching fractions $\mathcal{B}(B \rightarrow \chi_{c1}X)$ and $\mathcal{B}(B \rightarrow \chi_{c2}X)$ to be $(3.03 \pm 0.05 \pm 0.25) \times 10^{-3}$ and $(0.70 \pm 0.06 \pm 0.10) \times 10^{-3}$, respectively. First (second) error is statistical (systematic). Here, the systematic uncertainty dominates the measured branching fractions.

Figure 1 (b) shows the obtained distribution of the $D\mathcal{B}$ in bins of $p_{\chi_{cJ}}^*$. Suppression of two-body decay of χ_{c2} is visible in the $p_{\chi_{cJ}}^*$ distribution. Most of the χ_{c2} production comes from decays of three-body or more.

4 Exclusive reconstruction

The reconstructed invariant mass of the χ_{c1} (χ_{c2}) is required to satisfy $3.467 \text{ GeV}/c^2 < M_{J/\psi\gamma} < 3.535 \text{ GeV}/c^2$ ($3.535 \text{ GeV}/c^2 < M_{J/\psi\gamma} < 3.611 \text{ GeV}/c^2$). A mass-constrained fit is applied to the selected χ_{c1} and χ_{c2} candidates.

χ_{cJ} candidates are combined with charged kaon and pion candidate tracks to reconstruct B meson. To identify the B meson, two kinematical variables are used: beam-constrained mass (M_{bc}) and energy difference (ΔE). The M_{bc} is defined as $\sqrt{E_{\text{beam}}^2 - (\sum_i \vec{p}_i)^2}$ and the ΔE is defined as $\sum_i E_i - E_{\text{beam}}$, where E_{beam} is the beam energy in the CM frame and p_i (E_i) is the momentum (energy) of the i -th daughter particle in the CM frame and the summation is over all final states used for reconstruction. We reject candidates having M_{bc} less than $5.27 \text{ GeV}/c^2$ or $|\Delta E| > 120 \text{ MeV}$. We extract the signal yield from an unbinned extended maximum likelihood (UML) fit to the ΔE variable. Fig. 2 and 3 shows the fit to the ΔE distribution for the decay modes of interest.

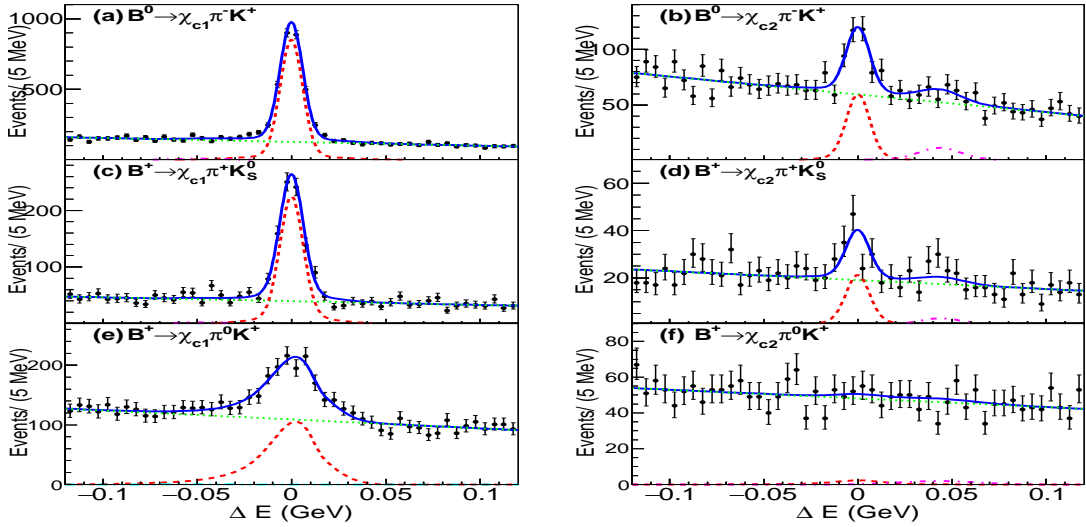


Figure 2: ΔE distribution for (a) $B^0 \rightarrow \chi_{c1} \pi^- K^+$, (b) $B^0 \rightarrow \chi_{c2} \pi^- K^+$, (c) $B^+ \rightarrow \chi_{c1} \pi^+ K_S^0$, (d) $B^+ \rightarrow \chi_{c2} \pi^+ K_S^0$, (e) $B^+ \rightarrow \chi_{c1} \pi^0 K^+$, and (f) $B^+ \rightarrow \chi_{c2} \pi^0 K^+$ decay modes. The curves show the signal (red dashed), peaking background (magenta dash-dotted) and the background component (green dotted for combinatorial) as well as the overall fit (blue solid).

To understand the production mechanism of intermediate states, we look at the background subtracted $M_{\chi_{cJ}\pi}$, $M_{K\pi}$, $M_{\chi_{cJ}\pi\pi}$, $M_{K\pi\pi}$, and $M_{\pi\pi}$ distributions for the decay mode of interest. We perform a UML fit to the ΔE distribution and use the $sPlot$ formalism [11] to project signal events in the distribution of interest.

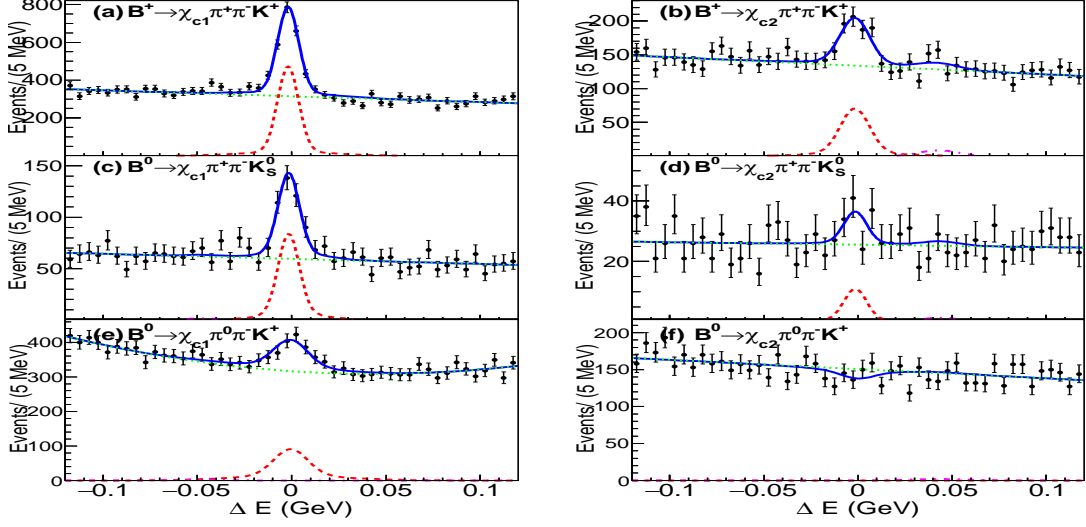


Figure 3: ΔE distributions for (a) $B^+ \rightarrow \chi_{c1} \pi^+ \pi^- K^+$, (b) $B^+ \rightarrow \chi_{c2} \pi^+ \pi^- K^+$, (c) $B^0 \rightarrow \chi_{c1} \pi^+ \pi^- K_S^0$, (d) $B^0 \rightarrow \chi_{c2} \pi^+ \pi^- K_S^0$, (e) $B^0 \rightarrow \chi_{c1} \pi^0 \pi^- K^+$ and (f) $B^0 \rightarrow \chi_{c2} \pi^0 \pi^- K^+$ decay modes. The curves show the signal (red dashed), peaking background (magenta dash-dotted) and the background component (green dotted for combinatorial) as well as the overall fit (blue solid).

The $K^*(892)$ is found to be a major contribution in the $B \rightarrow \chi_{c1} \pi K$ decay modes as seen from Fig. 4 (a), (e) and (i), while in $B \rightarrow \chi_{c2} \pi K$ decays the $K^*(892)$ component is less prominent. Our study suggests that the $B \rightarrow \chi_{c2} K^*(892)$ mechanism does not dominate the $B \rightarrow \chi_{c2} \pi K$ decay, which is in marked contrast to the χ_{c1} case. From this study one can say that the production mechanism of the χ_{c2} from B mesons is different in three-body decays for the $B \rightarrow \chi_{cJ} \pi K$ case.

Background subtracted $sPlot$ distribution of $M_{\chi_{cJ} \pi \pi}$, $M_{\chi_{cJ} \pi^\pm}$, $M_{K \pi \pi}$, $M_{K^+ \pi^-}$, and $M_{\pi^+ \pi^-}$ are shown in Figs. 5 and 6 for the $B^+ \rightarrow \chi_{cJ} \pi^+ \pi^- K^+$ decay mode. No narrow resonance is seen in the $M_{\chi_{cJ} \pi^+ \pi^-}$ and $M_{\chi_{cJ} \pi^\pm}$ distributions with the current statistics.

In our search for the $X(3872)$ and/or $\chi_{c1}(2P)$ decaying into $\chi_{c1} \pi^+ \pi^-$, we didn't find any signal and provided upper limit (@ 90% C.L.) as:

- $\mathcal{B}(B^\pm \rightarrow X(3872)K^\pm) \times \mathcal{B}(X(3872) \rightarrow \chi_{c1} \pi^+ \pi^-) < 1.4 \times 10^{-6}$
- $\mathcal{B}(B^+ \rightarrow \chi_{c1}(2P)K^+) \times \mathcal{B}(\chi_{c1}(2P) \rightarrow \chi_{c1}(1P)\pi^+ \pi^-) < 1.1 \times 10^{-5}$

5 Summary

Belle presented the preliminary results at this conference. We measured the direct branching fractions $\mathcal{B}(B \rightarrow \chi_{c1} X)$ and $\mathcal{B}(B \rightarrow \chi_{c2} X)$ to be $(3.03 \pm 0.05 \pm 0.25) \times 10^{-3}$

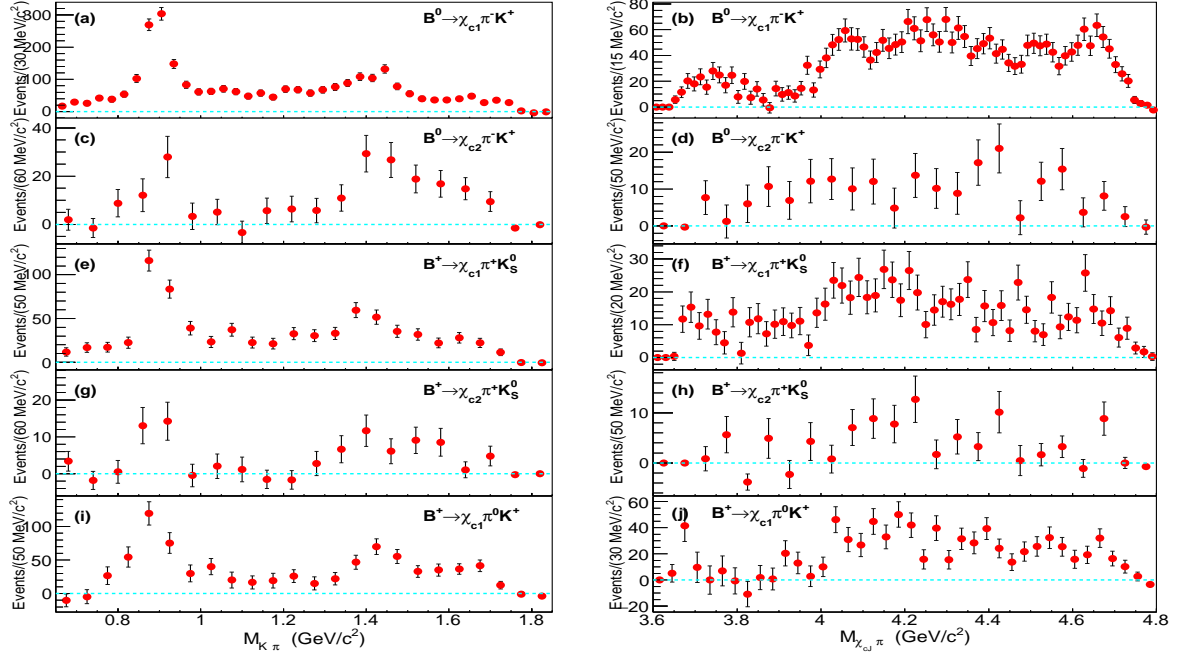


Figure 4: Background subtracted $s\mathcal{P}lot$ $M_{K\pi}$ and $M_{\chi_{cJ}\pi}$ distributions for (a and b) $B^0 \rightarrow \chi_{c1} \pi^- K^+$, (c and d) $B^0 \rightarrow \chi_{c2} \pi^- K^+$, (e and f) $B^- \rightarrow \chi_{c1} \pi^- K_S^0$, (g and h) $B^- \rightarrow \chi_{c2} \pi^- K_S^0$ and (i and j) $B^- \rightarrow \chi_{c1} \pi^0 K^+$ decay modes.

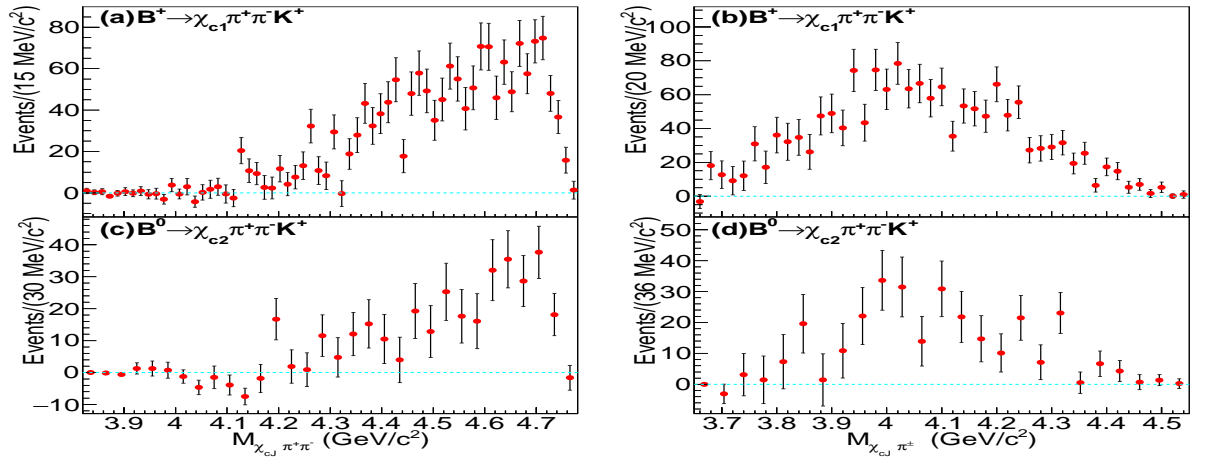


Figure 5: Background subtracted $s\mathcal{P}lot$ (a) $M_{\chi_{c1}\pi^+\pi^-}$, (b) $M_{\chi_{c1}\pi^\pm}$, (c) $M_{\chi_{c2}\pi^+\pi^-}$ and (d) $M_{\chi_{c2}\pi^\pm}$ distributions for $B^+ \rightarrow \chi_{cJ} \pi^+ \pi^- K^+$ decay modes.

Table 1: Summary of the results. Signal yield (Y) from the fit, significance (\mathcal{S}) with systematics included, corrected efficiency (ϵ) and measured \mathcal{B} . For \mathcal{B} , the first (second) error is statistical (systematic). Here, in the neutral B decay case, the $K_S^0 \rightarrow \pi^+\pi^-$ branching fraction is included in the efficiency (ϵ) but the factor of 2 (for $K^0 \rightarrow K_S^0$ or K_L^0) is taken into account separately. $\mathcal{R}_{\mathcal{B}}$ is the ratio of $\mathcal{B}(B \rightarrow \chi_{c2}X)$ to $\mathcal{B}(B \rightarrow \chi_{c1}X)$, where X is the same set of particles accompanying the χ_{c1} (χ_{c2}) in the final states.

Decay	Yield (Y)	$\mathcal{S}(\sigma)$	$\epsilon(\%)$	$\mathcal{B} (10^{-4})$	$\mathcal{R}_{\mathcal{B}}$
$B^0 \rightarrow \chi_{cJ}\pi^-K^+$					0.14 ± 0.02
χ_{c1}	2774 ± 66	66.7	17.9	$4.97 \pm 0.12 \pm 0.28$	
χ_{c2}	206 ± 25	8.7	16.2	$0.72 \pm 0.09 \pm 0.05$	
$B^+ \rightarrow \chi_{cJ}\pi^+K^0$					0.20 ± 0.04
χ_{c1}	770 ± 35	33.7	8.6	$5.75 \pm 0.26 \pm 0.32$	
χ_{c2}	76.4 ± 14.7	4.6	7.5	$1.16 \pm 0.22 \pm 0.12$	
$B^+ \rightarrow \chi_{cJ}\pi^0K^+$					< 0.21
χ_{c1}	803 ± 70	15.6	7.8	$3.29 \pm 0.29 \pm 0.19$	
χ_{c2}	17.5 ± 28.4	0.4	7.0	< 0.62	
$B^+ \rightarrow \chi_{cJ}\pi^+\pi^-K^+$					0.36 ± 0.05
χ_{c1}	1502 ± 70	19.2	12.8	$3.74 \pm 0.18 \pm 0.24$	
χ_{c2}	269 ± 34	8.4	11.4	$1.34 \pm 0.17 \pm 0.09$	
$B^0 \rightarrow \chi_{cJ}\pi^+\pi^-K^0$					< 0.61
χ_{c1}	268 ± 30	7.1	5.4	$3.16 \pm 0.35 \pm 0.32$	
χ_{c2}	37.8 ± 14.2	1.8	4.8	< 1.70	
$B^0 \rightarrow \chi_{cJ}\pi^0\pi^-K^+$					< 0.25
χ_{c1}	545 ± 81	6.5	5.0	$3.52 \pm 0.52 \pm 0.24$	
χ_{c2}	-76.7 ± 42.0	-	4.3	< 0.74	

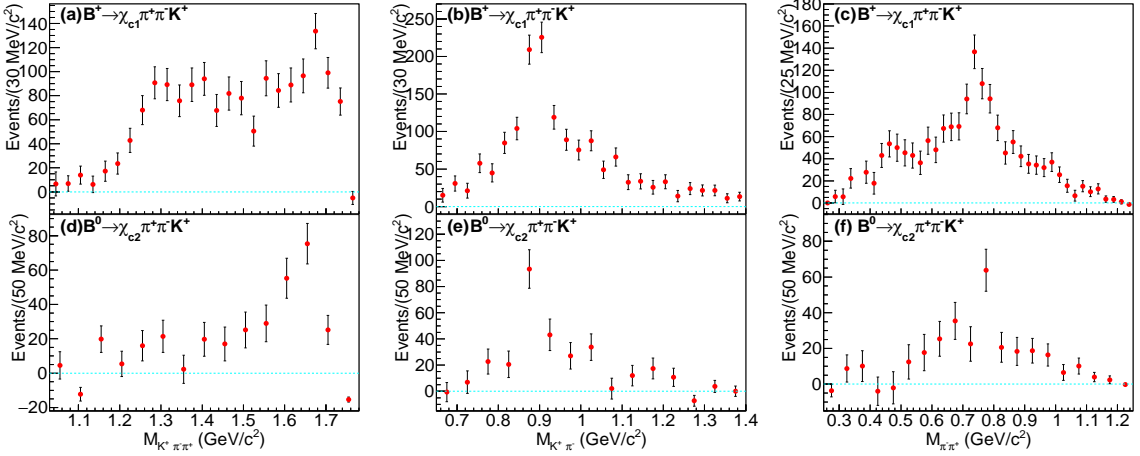


Figure 6: Background subtracted $sPlot$ (a and d) $M_{K^+\pi^+\pi^-}$, (b and e) $M_{K^+\pi^-}$ and (c and f) $M_{\pi^+\pi^+}$ distributions for $B^+ \rightarrow \chi_{c1}\pi^+\pi^-K^+$ decay (upper) and $B^+ \rightarrow \chi_{c2}\pi^+\pi^-K^+$ decay (lower), respectively.

and $(0.70 \pm 0.06 \pm 0.10) \times 10^{-3}$, respectively. We observe the $B^0 \rightarrow \chi_{c2}\pi^-K^+$ decay mode for the first time, with 206 ± 25 signal events having a 8.7σ significance, along with evidence for the $B^+ \rightarrow \chi_{c2}\pi^+K_S^0$ decay mode, with 76 ± 15 signal events and a significance of 4.6σ . In four-body decays, we observe the $B^+ \rightarrow \chi_{c1}\pi^+\pi^-K^+$, $B^+ \rightarrow \chi_{c1}\pi^+\pi^-K^+$, $B^0 \rightarrow \chi_{c1}\pi^+\pi^-K_S^0$, and $B^0 \rightarrow \chi_{c1}\pi^0\pi^-K^+$ decay modes for the first time and report on measurements of their branching fractions. We find that χ_{c2} production in comparison with χ_{c1} increases with a higher number of multi-body B decays. We observe that the χ_{c2} is more often accompanied by higher K^* resonances as opposed the χ_{c1} which is dominantly produced with lower K^* resonance. Inclusive and exclusive study of B decays having χ_{c2} in the final state suggests suppression of two-body B decay due to suppression of a tensor, while multi-body B decays into χ_{c2} are allowed. In our search for $X(3872) \rightarrow \chi_{c1}\pi^+\pi^-$ and $\chi_{c1}(2P)$, we determine an U.L. on the product of branching fractions. The negative result for our searches is compatible with the interpretation of $X(3872)$ as an admixture state of a $D^0\bar{D}^{*0}$ molecule and a $\chi_{c1}(2P)$ charmonium state.

ACKNOWLEDGEMENTS

We like to thank KEKB and all members of Belle collaboration along with their supporting funding agencies. This work is supported by a Grant-in-Aids from MEXT for Scientific Research on Innovative Areas (“Elucidation of New Hadrons with a Variety of Flavors”) and the U.S. Department of Energy and the National Science Foundation.

References

- [1] K. Abe *et al.* (Belle Collaboration), Phys. Rev. Lett. **89**, 011803 (2002).
- [2] B. Aubert *et al.* (BaBar Collaboration), Phys. Rev. D **67**, 032002 (2003).
- [3] N. Soni *et al.* (Belle Collaboration), Phys. Lett. B **634**, 155 (2006).
- [4] B. Aubert *et al.* (Babar Collaboration), Phys. Rev. Lett. **102**, 132001 (2009).
- [5] V. Bhardwaj *et al.* (Belle Collaboration), Phys. Rev. Lett. **107**, 091803 (2011).
- [6] Hereinafter, χ_{cJ} refers to either χ_{c1} or χ_{c2} , depending on which is reconstructed.
- [7] Charge-conjugate and neutral modes are included throughout the paper unless stated otherwise.
- [8] A. Abashian *et al.* (Belle Collaboration), Nucl. Instrum. Methods Phys. Res., Sect. A **479**, 117 (2002); also see detector section in J. Brodzicka *et al.*, Prog. Theor. Exp. Phys. (2012) 04D001.
- [9] S. Kurokawa and E. Kikutani, Nucl. Instrum. Methods Phys. Res., Sect. A **499**, 1 (2003), and other papers included in this Volume; T. Abe *et al.*, Prog. Theor. Exp. Phys. (2013) 03A001 and following articles up to 03A011.
- [10] P. Koppenburg *et al.* (Belle Collaboration), Phys. Rev. Lett. **93**, 061803 (2004).
- [11] M. Pivk and F.R.Le Diberder, Nucl. Instrum. Methods Phys. Res., Sect. A **555**, 356 (2005).